



OPEN ACCESS

EDITED BY
Peng Jin,
University of Guangzhou, China

REVIEWED BY
Yahe Li,
Ningbo University, China
Wei Liu,
Shanghai University, China
Guang Gao,
Xiamen University, China

*CORRESPONDENCE
Fang Yan
✉ yf_dolphin@163.com
Tingzhu Yuan
✉ zlt2020@163.com

†These authors have contributed
equally to this work and share
first authorship

RECEIVED 21 April 2024
ACCEPTED 24 May 2024
PUBLISHED 06 June 2024

CITATION
Li B, Xu Z, Jiang X, Wu H, Bao M,
Zang S, Yan F and Yuan T (2024)
Diverse nitrogen enrichments enhance
photosynthetic resistance of *Sargassum
horneri* to ultraviolet radiation.
Front. Mar. Sci. 11:1420839.
doi: 10.3389/fmars.2024.1420839

COPYRIGHT
© 2024 Li, Xu, Jiang, Wu, Bao, Zang, Yan and
Yuan. This is an open-access article distributed
under the terms of the [Creative Commons
Attribution License \(CC BY\)](https://creativecommons.org/licenses/by/4.0/). The use,
distribution or reproduction in other forums
is permitted, provided the original author(s)
and the copyright owner(s) are credited and
that the original publication in this journal is
cited, in accordance with accepted academic
practice. No use, distribution or reproduction
is permitted which does not comply with
these terms.

Diverse nitrogen enrichments enhance photosynthetic resistance of *Sargassum horneri* to ultraviolet radiation

Baoqi Li^{1†}, Zhiguang Xu^{1†}, Xiaotong Jiang¹, Hongyan Wu¹,
Menglin Bao¹, Shasha Zang¹, Fang Yan^{1*} and Tingzhu Yuan^{2*}

¹School of Life Sciences, Ludong University, Yantai, China, ²Marine Economy Promotion Center, Marine Ecological Civilization Comprehensive Experimental Area of Changdao, Yantai, China

In recent years, golden tides caused by floating *Sargassum* have induced severe ecological disasters globally. Eutrophication is a significant factor contributing to the massive spread of *Sargassum* golden tides. Furthermore, the thalli of *Sargassum* that float on the ocean surface are subjected to more ultraviolet radiation (UVR). The coupled impact of eutrophication and UVR on the photosynthetic physiology of golden tide species remains unclear. In this study, the thalli of *Sargassum horneri*, known to cause golden tide, were cultured and acclimated to three distinct nitrogen (N) conditions (natural seawater, NSW; NH₄⁺-N enrichment; and NO₃⁻-N enrichment) for 6 days. Subsequently, the thalli were exposed to two different radiation treatments (photosynthetically active radiation (150 W m⁻²), PAR, 400–700 nm; PAR (150 W m⁻²) + UVR (28 W m⁻²), 280–700 nm) for 120 min, to investigate the photosynthetic effects of UVR and N on this alga. The findings demonstrated that exposure to UVR impeded the photosynthetic capacity of *S. horneri*, as evidenced by a decrease in the maximum photochemical quantum yield (F_v/F_m), photosynthetic efficiency (α) and chlorophyll content. Under diverse N-enrichment conditions, the alga tended to adopt various strategies to mitigate the adverse effects of UVR. NH₄⁺-enrichment dissipated excess UVR energy through a greater increase in non-photochemical quenching (NPQ). While NO₃⁻ enrichment protected alga by enhancing N assimilation (higher nitrate reductase activity (NRA) and soluble protein content), and maintained a stable energy captured per unit reaction center for electron transfer (ET₀/RC) and a higher net photosynthetic rate. Although different N enrichments could not completely offset the damage caused by UV radiation, they secured the photoprotective ability of *S. horneri* in several ways.

KEYWORDS

Sargassum horneri, nitrogen source, ultraviolet radiation, chlorophyll fluorescence, photodamage protection

1 Introduction

Golden tides are characterized by the explosive growth of *Sargassum* seaweeds after they detach and float on the surface of the sea (Smetacek and Zingone, 2013). Since the 21st century, the Caribbean, West Africa, and Gulf of Mexico have witnessed the emergence of gold tides in the species *Sargassum fluitans* (*S. fluitans*) and *Sargassum natans* (*S. natans*) (Schell et al., 2015; Van Tussenbroek et al., 2017; Wang et al., 2019). Golden tides of *S. horneri* have also been recorded in the East China Sea, Yellow Sea, and South Korea (Hwang et al., 2016; Qi et al., 2017; Xing et al., 2017; Liu et al., 2018). The decay of algae following golden tide outbreaks leads to the release of toxic substances that negatively impact local marine ecosystems (Caselle et al., 2018) and, consequently, affects fisheries, aquaculture, and coastal tourism in the area (Williams and Feagin, 2010; Zhang et al., 2019). The highly frequent occurrence of golden tides has garnered the interest of various segments of society (Byeon et al., 2019; Xiao et al., 2021).

Human-induced ozone holes have led to more UVR reaching Earth's surface. Although studies have shown that the size of ozone holes has been decreasing since 2010 (Solomon et al., 2016), a hole three times the size of Greenland was observed over the Arctic in 2020 (Witze, 2020). The enhancement of UVR was expected to continue for some time (Bais et al., 2015). UVR can significantly reduce the growth and pigmentation of macroalgae (Gao and Xu, 2008; Schmidt et al., 2010), impede electron transfer rates, and reduce maximum photochemical quantum yield (Gao et al., 2019). UVR increases the permeability of cell membranes (Sobrinho et al., 2004), damages proteins and DNA molecules (Ruhland et al., 2007). Furthermore, it can lead to cell death (Agustí and Llabrés, 2007). Macroalgae have evolved various photoprotective mechanisms to mitigate the detrimental effects of UVR, such as the production of UV-absorbing compounds (Mayalen et al., 2009; Rautio and Tartarotti, 2010), heightened non-photochemical quenching to dissipate excess light energy (Goss and Lepetit, 2015), accelerated synthesis and interconversion of D1 proteins (Wu et al., 2011), enhancement of antioxidant system efficiency (Xu et al., 2022), and various other adaptations. During the golden tide, the lack of seawater shielding results in increased exposure of seaweeds floating near the water surface to UVR (Tedetti and Sempère, 2006). However, there is currently a dearth of research on the response of golden tide algae to UVR.

In recent years, rapid economic development has resulted in increased nutrient inputs to global coasts (Neori et al., 2004), leading to a more serious eutrophication problem that poses a growing threat to coastal ecosystems (Bricker et al., 2008). Nitrogen (N) is a crucial element required for the growth of macroalgae (Paliwal et al., 2017). The concentration of N in natural seawater is typically low and subject to significant seasonal variation, which often constitutes a limiting factor for the growth of macroalgae (Hwang et al., 2004). In general, N deficiency exacerbates the detrimental effects of UVR on algal photosynthesis (Davison et al., 2007). However, an adequate supply of nitrate-N (Xu et al., 2023a) for *S. horneri* or ammonia-N (Xu and Gao, 2012) for *Gracilaria lemaneiformis* tends to mitigate this inhibitory effect on

photosynthesis. Macroalgae can absorb a diverse array of inorganic and organic forms of N, with NO_3^- and NH_4^+ as the primary sources of N. Variations in the uptake and utilization of these N sources frequently lead to disparities in physiological processes, including growth, biochemical constituents, and nutrient uptake in macroalgae (Sun et al., 2015). The growth rates of *Porphyra haiyanensis* and *Porphyra yezoensis* are higher under NH_4^+ -N treatments, whereas *Porphyra leucostica* exhibits better growth in NO_3^- -N environments (Carmona et al., 2006). However, the precise similarities and differences in the roles of various N sources in the response of *S. horneri* to UV stress remain unclear.

S. horneri, a species of Heterokontophyta phylum, Fucales order, Sargassaceae family, and *Sargassum* genus, is widely distributed along the western coast of the Pacific Ocean and plays a crucial role in coastal seaweed ecosystems. It provides habitat, baiting, and reproduction sites for various marine organisms (Terawaki et al., 2003). Due to its high adaptability and rapid growth, *S. horneri* often becomes an invasive species (Sfriso and Facca, 2013), affecting local ecosystems (Byeon et al., 2019). *Sargassum* golden tides were observed off the northern coast of Taiwan Island in China in 2012 (Komatsu et al., 2014) and offshore Jiangsu Province in China in 2017 (Zhuang et al., 2021). Eutrophication serves as a critical trigger for the emergence of golden tide blooms, which tend to occur in eutrophic offshore or upwelling waters characterized by elevated NO_3^- -N concentrations (Smetacek and Zingone, 2013; Wang et al., 2019). In coastal regions, mariculture generates wastewater, primarily from fish excrement and feed residues, which typically contain high levels of N (primarily in the form of NH_4^+ -N), phosphorus (P), and suspended solids (Song et al., 2018). Considering that floating *S. horneri* exposed to more UVR frequently blooms in eutrophic waters, we speculate that both enrichments of NO_3^- -N and NH_4^+ -N in eutrophication may enormously alleviate the stress of UVR on the photosynthesis of this alga. To verify this hypothesis, the effects of UVR and different N enrichments (NO_3^- -N and NH_4^+ -N) on the photosynthetic activity of this alga were examined, and some protection strategies related to energy capture, absorption, transfer, and heat dissipation were also partially investigated in this study. The aim was to provide evidence to support the underlying mechanism responsible for the formation of *Sargassum* golden tides in eutrophic seawater.

2 Materials and methods

2.1 Materials

In April 2022, *S. horneri* was sampled from a natural population in Lidao Bay, Rongcheng City, Shandong Province (37°15' N, 122° 35' E). The collected samples were transported to the laboratory within 2 h in a low-temperature incubator set at 5°C. Healthy and uniform individuals were selected and cleaned using autoclaved seawater to remove algae attached microorganisms. To eliminate the influence of transportation process, thalli were precultured in natural seawater (salinity: 28 psu) in illumination incubator (MGC-

250P, Yiheng Technical Co. Ltd. Shanghai, China) for 24 h. Referring to Dai et al. (2024), the photosynthetically active radiation (PAR) provided by LED tubes was set at $100 \mu\text{mol photons m}^{-2} \text{s}^{-1}$ with a light and dark period of 12 h:12 h, and the temperature was maintained at 18°C . Culture media were aerated continuously with ambient air at a rate of 2 L min^{-1} . After 24-h preculture, algae were used for subsequent experiments.

2.2 Experimental design

Referencing to the N concentration in seawater during *S. horneri* gold tide (Qi et al., 2017), three distinct N treatments were established by incorporating NaNO_3 or NH_4Cl liquor into the natural seawater.

- (1) Natural seawater (NSW): The $\text{NO}_3^- \text{N}$ concentration was $5 \mu\text{mol L}^{-1}$, and the $\text{NH}_4^+ \text{N}$ concentration was $1.7 \mu\text{mol L}^{-1}$;
- (2) $\text{NH}_4^+ \text{N}$ enriched seawater (NH_4^+): NH_4Cl was added to the natural seawater to a final concentration of $200 \mu\text{mol L}^{-1}$ of total inorganic N.
- (3) $\text{NO}_3^- \text{N}$ enriched seawater (NO_3^-): NaNO_3 was added to the natural seawater until the final concentration of total inorganic N was $200 \mu\text{mol L}^{-1}$.

The inorganic P concentration was set at $15 \mu\text{mol L}^{-1}$ in all treatments through the addition of NaH_2PO_4 to prevent P limitation during the experiment. Moreover, the seawater was replaced every two days, while the remaining conditions were the same as those employed in the temporary culture.

Daily measurements of the maximum photochemical quantum yield (F_v/F_m) of algae were performed to ensure their healthy state. Following six consecutive days of incubation, the F_v/F_m of the thalli stabilized (Supplementary Figure S1A), which served as evidence that *S. horneri* had acclimated to the incubation environment.

Two radiation treatments were obtained using a solar simulator (Sol 1200, Hönle GmbH, Germany) and two types of filters

(Nantong, China), and the emission spectrum of the solar simulator compared with sunlight and transmittance of two types of filter were shown in Figure 1. Thalli that were cultivated under various conditions of N acclimatization were exposed to two radiation treatments, PAR ($400\text{--}700 \text{ nm}$, 150 W m^{-2}) and PAR+UVR ($280\text{--}700 \text{ nm}$, $150 \text{ W m}^{-2} + 28 \text{ W m}^{-2}$), for 2 h to simulate the high UVR on the seawater surface in the afternoon (Xu et al., 2023a, Xu et al., 2023b). The irradiance levels were set according to the radiation on the sea surface when the golden tide of *S. horneri* bloomed (Qi et al., 2017; Xu et al., 2022), and measured by a radiometer (PMA 2100, Solar Light, USA). During culture, the quartz tubes with thalli were placed in a water bath, and the temperature was controlled at 18°C by a low-temperature thermostatic bath (YRDC-0506, Yarong, China).

- (1) PAR treatment: The quartz tubes were covered with ZJB-400 filters, which effectively blocked solar radiation below 400 nm , thereby restricting the thalli within the tubes to receive PAR only within the range of $400\text{--}700 \text{ nm}$.
- (2) PAR+UVR treatment: The quartz tubes were covered with ZJB-280 filters, thereby exposing the thalli to photons in the PAR+UVA+UVB range ($280\text{--}700 \text{ nm}$).

The relevant photosynthetic indices were then measured.

2.3 F_v/F_m and NPQ determination

The maximum photochemical quantum yield (F_v/F_m) and non-photochemical quenching (NPQ) were determined using a hand-held chlorophyll fluorometer (AP-C100, Photon Systems Instruments, Czech Republic) to measure the fluorescence of 0.1 g fresh weight (FW) of algae thalli that had been exposed to different radiation treatments for 2 h and then dark-adapted for 15 min in a dark environment. F_v/F_m also was measured during the process of pre-acclimation for difference N enrichments. The F_v/F_m and NPQ values were calculated using the following equations (Lacour et al., 2023):

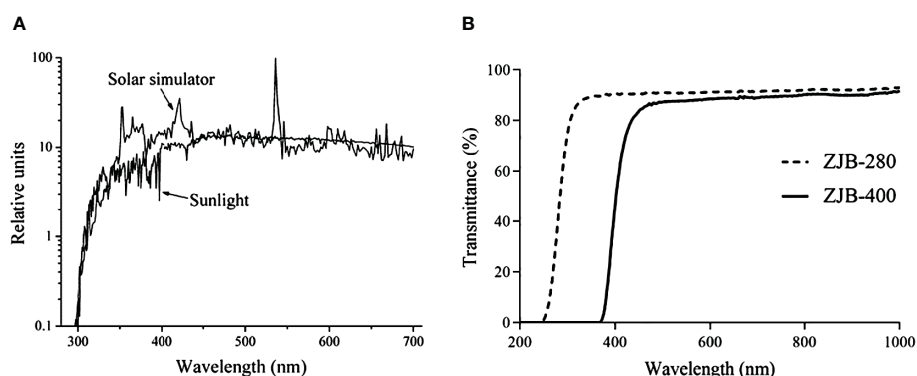


FIGURE 1
The emission spectrum of the solar simulator compared with sunlight (A) and transmittance of two types of filters (B).

$$(F_v/F_m) = (F_m - F_o)/F_m$$

$$NPQ = (F_m - F_m')/F_m'$$

Where F_o is the minimum fluorescence under dark adaptation with a light source irradiance (approximately $0.15 \mu\text{mol photons m}^{-2} \text{ s}^{-1}$), F_m is the maximum fluorescence was obtained with a saturated light ($4000 \mu\text{mol photons m}^{-2} \text{ s}^{-1}$) in the dark-adapted state. The maximum fluorescence (F_m') of the algae in the light-adapted state was measured using saturated light ($4000 \mu\text{mol photons m}^{-2} \text{ s}^{-1}$).

2.4 Determination of rapid chlorophyll fluorescence induction and JIP test

Radiation-treated algae (0.1 g FW) was subjected to a 15-min period of dark acclimation, after which the fast chlorophyll fluorescence induction curve (OJIP curve) of the algae was determined using a double-modulation chlorophyll fluorometer (FL6000, Photon Systems Instruments, Czech Republic). The fluorescence signals were recorded with a scanning time that ranged from $10 \mu\text{s}$ to 2 s and were labeled as O, J (at about 2 ms), I (at about 30 ms), and P. To show the obvious OJIP phase, the horizontal coordinate time was changed to a logarithmic form to directly observe the J and I points and infer the state of the PSII reaction center. The OJIP curve provides information on the light energy absorbed per unit reaction center (ABS/RC), the light energy dissipated (DI_0/RC), the energy captured per unit reaction center for the reduction of QA (TR_0/RC), the energy captured per unit reaction center for electron transfer (ET_0/RC), the degree of closure of active reaction centers at 2 ms (V_j), the initial slope (M_0), and the degree of opening of active reaction centers at 2 ms (Ψ_0). These parameters were calculated according to the method described by [Strasser et al. \(2000\)](#).

$$V_j = (F_j - F_o)/(F_m - F_o)$$

$$M_0 = 4 \times (F_{300\mu\text{s}} - F_o)/(F_m - F_o)$$

$$\Psi_0 = 1 - V_j$$

$$ABS/RC = M_0 \times (1/V_j) \times (1/\phi_{P_0})$$

$$TR_0/RC = M_0 \times (1/V_j)$$

$$ET_0/RC = M_0 \times (1/V_j) \times \Psi_0$$

$$DI_0/RC = (ABS/RC) - (TR_0/RC)$$

2.5 Determination of photosynthetic pigment and UV-absorbing compound contents

After 2-h radiation exposure, thalli (0.2 g FW) were homogenized with a methanol solution and fixed with 10 mL of the solution. The mixture was kept at 4°C for 24 h in the dark and then centrifuged at 4°C for 10 min at 5000 rpm. The absorbance of the supernatant was measured at wavelengths ranging from 250 to 750 nm using an ultraviolet spectrophotometer (UH-5300, Hitachi, Japan), and the photosynthetic pigment contents were calculated according to [Xu and Gao \(2012\)](#).

The relative content of UV-absorbing compounds (UVACs) was expressed as the ratio of the peak height (H) at 340 nm of the absorption curve in the UV region to FW of the algae ([Helbling et al., 2004](#)).

2.6 Measurement of net photosynthetic rate

A portable photosynthesizer (TARGAS-1, Lufthansa Technik Group Ltd., USA) was utilized to measure net photosynthetic rate. Following a 2-h treatment with varying UV radiation, thalli (0.2 g FW) were taken and placed in the reaction chamber of the photosynthesizer for 10-min measurement. The chamber's area was set to 1 cm^2 , the temperature set to 18°C , and the light level provided by LED tubes was set to $700 \mu\text{mol photons m}^{-2} \text{ s}^{-1}$, according to radiation treatments of PAR and PAR+UVR. The net photosynthetic rate of the algae was expressed as the rate of CO_2 reduction per unit time in the reaction chamber of the photosynthesizer ($\mu\text{mol CO}_2 \text{ s}^{-1} \text{ g}^{-1}$). The CO_2 concentration at the beginning of measurement is the ambient concentration (400 ppmv).

2.7 Measurement of nitrate reductase activity

The nitrate reductase (NR) activity was assayed in thalli under different radiation or N treatments, according to [Corzo and Niell \(1991\)](#) and [Anibal et al. \(2014\)](#). A total of 0.1 g FW radiation-treated algae was added to a reaction medium solution comprised of 0.1 mol L^{-1} phosphate buffer (pH 7.5), $10 \mu\text{mol L}^{-1}$ glucose, 1 mmol L^{-1} EDTA, 200 mmol L^{-1} NaNO_3 , and 0.1% propanol. In the reaction solution, O_2 was removed by charging N_2 for 2 min to prevent the generated NO_2^- from being oxidized to NO_3^- . The reaction was then allowed to proceed at 30°C for 1 h in the dark. The alga was removed from the reaction solution and the amount of NO_2^- generated in the solution was measured. The amount of NO_2^- generated by the alga per unit time was utilized to express the nitrate reductase activity ($\mu\text{g g}^{-1} \text{ h}^{-1}$).

2.8 Determination of soluble protein content

A total of 0.5 g FW of the thalli was collected, ground by adding distilled water to a mortar, mixed, and subsequently centrifuged at 4000 rpm for 10 min. The concentration of soluble proteins in the extract was determined by the Bradford method (Bradford, 1976).

$$\text{soluble protein content (mg g}^{-1}\text{)} = (M \times V)/(1000 \times W)$$

where M is the soluble protein concentration of the extract ($\mu\text{g mL}^{-1}$), V denotes 10 mL of the extract, and W is the FW of the algae (g).

2.9 Measurement of soluble carbohydrates content

At the end of the experiment, approximately 0.2 g of FW thalli from each culture condition was ground using a mortar and distilled water. The extraction solution was heated in a water bath at 70°C for 30 min. After cooling the extract to room temperature, it was centrifuged at 4000 rpm for 10 min. The concentration of soluble carbohydrates in the extract was determined using the phenol-sulfuric acid method (Kochert, 1978), and the soluble carbohydrate content was calculated as follows:

$$\text{soluble carbohydrate content (mg g}^{-1}\text{)} = (M \times V)/(1000 \times W)$$

where M is the soluble carbohydrate concentration ($\mu\text{g mL}^{-1}$), V is the 25 mL extract, and W is the FW of the algae (g).

2.10 Data analysis

All the measurement results were expressed as mean \pm SD ($n \geq 3$). Data were analyzed and organized using Excel and SPSS 24.0,

and graphs were created using GraphPad Prism 8 and Origin 2021. All data conform to normality test and variance homogeneity test. Two-way ANOVA (Duncan) was performed to analyze the interaction between N and UV radiation, with a significance level of $P < 0.05$. Two-way ANOVA analysis results were presented in 'Supplementary Material' (Supplementary Table S1 for F_v/F_m and NPQ; Supplementary Table S2 for V_j , M_0 , Ψ_0 , ABS/RC, TR_0 /RC, DI_0 /RC, and ET_0 /RC; Supplementary Table S3 for Chla, Car, and UVACs; Supplementary Table S4 for net photosynthetic rate; Supplementary Table S5 for nitrate reductase activity; Supplementary Table S6 for soluble protein and soluble carbohydrates). After two-way ANOVA analysis, we conducted independent sample t test for the UV radiation and one-way ANOVA for the nitrogen source. In the graphs, different lowercase letters indicate significant differences between treatments. The symbol * indicates significant differences between the UV radiation treatments.

3 Results

3.1 Maximum photochemical quantum yield (F_v/F_m) and non-photochemical quenching

The effects of various N acclimations followed by UV radiation treatments on F_v/F_m and non-photochemical quenching (NPQ) of *S. horneri* are illustrated in Figure 2. The results of the two-way analysis of variance (ANOVA) indicated that UV radiation had a significant independent effect on F_v/F_m ($P = 0.003$). The exposure to UV radiation for 2 h resulted in a significant reduction in the F_v/F_m of *S. horneri* under PAR+UVR treatment compared with PAR treatment ($P < 0.05$). Specifically, under the PAR+UVR treatment, the F_v/F_m of *S. horneri* treated with natural, NH_4^+ -N-enriched, and NO_3^- -N-enriched seawater cultures were 72.22%, 64.02%, and 67.78%, respectively, lower than that of the PAR treatment.

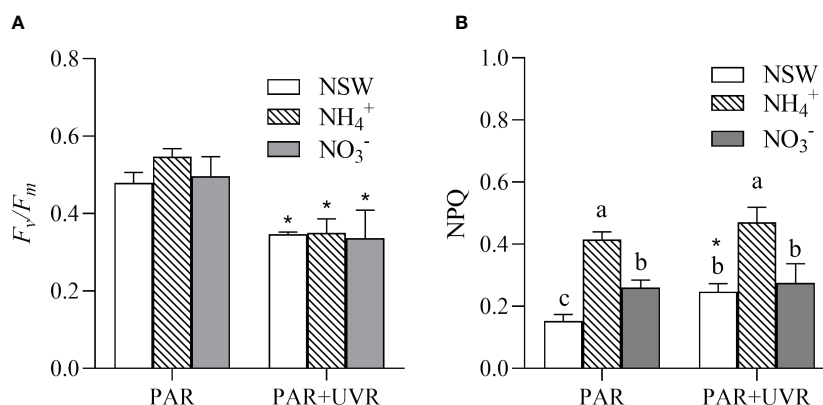


FIGURE 2 Effects of 2-h UV radiation treatments on the maximum photochemical quantum yield (F_v/F_m , **A**) and non-photochemical quenching (NPQ, **B**) of *S. horneri* after grown under different N conditions for 6 days. NSW, natural seawater culture; NH_4^+ : NH_4^+ -N-enriched culture; NO_3^- : NO_3^- -N-enriched culture. Different letters above the error bars indicate significant differences between the different N-source treatments ($P < 0.05$, one-way ANOVA). The symbol * indicates significant differences between the UV radiation treatments ($P < 0.05$, t -tests). Vertical bars represent \pm SD of the means ($n = 3$).

The effects of UV radiation and N on the NPQ of *S. horneri* were independent ($P = 0.009$ for UV radiation, $P = 0.001$ for N), without significant interaction between them ($P = 0.225$). Under natural seawater culture conditions, UVR significantly increased the NPQ of *S. horneri* to 1.62 times that of the PAR treatment (Figure 2B). In contrast, under $\text{NH}_4^+\text{-N}$ and $\text{NO}_3^-\text{-N}$ -enriched culture conditions, there was no significant difference between the PAR and PAR+UVR treatments ($P > 0.05$). Under the same UV radiation conditions, N enrichment also elevated the NPQ of *S. horneri*. When the cultures were enriched with $\text{NH}_4^+\text{-N}$ or $\text{NO}_3^-\text{-N}$, the NPQ of *S. horneri* was 2.72 and 1.71 times higher, respectively, than that of the natural seawater culture under PAR treatment, and 1.90 and 1.12 times higher, respectively, than that of the natural seawater culture under PAR + UVR treatment. Furthermore, the NPQ of *S. horneri* cultured with $\text{NH}_4^+\text{-N}$ enrichment was significantly higher than that cultured with $\text{NO}_3^-\text{-N}$ enrichment in both UV radiation treatments ($P < 0.05$).

3.2 Rapid chlorophyll fluorescence induction and JIP test

The chlorophyll fluorescence induction curves of OJIP for N-adapted *S. horneri* after various UV radiation treatments are depicted in Figure 3. The O phase of *S. horneri* in natural seawater following PAR+UVR radiation was higher than that of the other treatments, suggesting that UVR radiation reduced the number of active reaction centers in the photosystem II (PSII). Under N enrichment conditions, UVR treatment resulted in significantly lower fluorescence in the O, J, I, and P phases in *S. horneri* than PAR treatment.

There was no significant effect of different forms of N and UV radiation on the V_j , M_0 , and Ψ_0 of *S. horneri* ($P > 0.05$). Furthermore, there was no significant interaction between UV radiation and N condition ($P > 0.05$). Under natural seawater culture conditions, the PAR+UVR treatment resulted in a significant increase in the V_j of *S. horneri* by 23.66% compared with the PAR treatment. However, under N enrichment conditions, there was no significant difference between the PAR+UVR and PAR treatments ($P > 0.05$). Additionally, there were no substantial differences in M_0 and Ψ_0 caused by different N form enrichments or UV radiation treatments ($P > 0.05$).

There was a significant main effect of both UV radiation and different N forms on ABS/RC ($P = 0.001$ for radiation, $P = 0.001$ for N) and DI_0/RC ($P = 0.001$ for radiation, $P = 0.001$ for N). Additionally, there also were significant interaction effects between UV radiation and N on both ABS/RC ($P = 0.001$) and DI_0/RC ($P = 0.001$). However, no significant main effect ($P > 0.05$) was observed for TR_0/RC and ET_0/RC . Under natural seawater culture, UVR increased the ABS/RC and DI_0/RC of *S. horneri* by 2.30 and 2.94 times, respectively, compared to the PAR-treated group. In the context of $\text{NO}_3^-\text{-N}$ enrichment, PAR+UVR treatment elevated the levels of ABS/RC and DI_0/RC by 44.98% and 69.97%, respectively, compared with PAR treatment. However, no such differences were observed in the $\text{NH}_4^+\text{-N}$ -enriched culture ($P > 0.05$). Furthermore, under PAR+UVR treatment conditions, the ABS/RC of *S. horneri* in the natural seawater culture was observed to be 2.07 and 1.47 times higher than that of $\text{NH}_4^+\text{-N}$ -enriched and $\text{NO}_3^-\text{-N}$ -enriched cultures, respectively. Additionally, the levels of DI_0/RC in $\text{NH}_4^+\text{-N}$ -enriched and $\text{NO}_3^-\text{-N}$ -enriched cultures increased by 145.43 and 56.81%, respectively, compared with natural seawater, and these differences were statistically significant

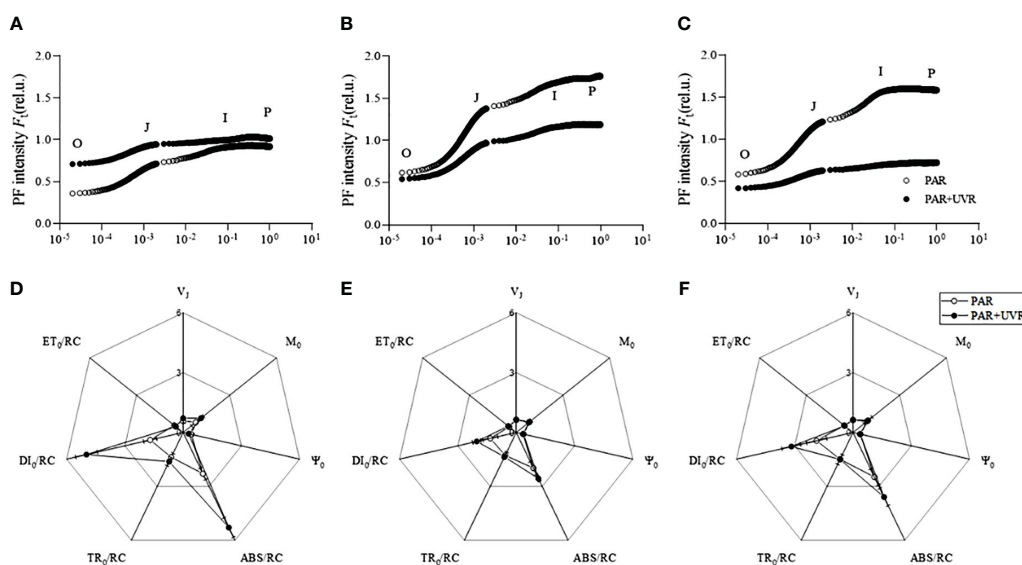


FIGURE 3
OJIP curves of *S. horneri* cultured in natural seawater (A), ammonia-enriched (B), and nitrate-enriched (C) with different UV radiation treatments, and relative variable fluorescence (V_j), initial slope of the OJIP fluorescence induction curve (M_0), degree of opening of active reaction centers (Ψ_0), energy fluxes for absorption per reaction center (ABS/RC), energy fluxes for trapping per reaction center (TR_0/RC), energy fluxes for dissipation per reaction center (DI_0/RC), and energy fluxes for electron transfer from Q_A to Q_A^- per reaction center (ET_0/RC) of *S. horneri* in cultures incubated in natural seawater (D), $\text{NH}_4^+\text{-N}$ -enriched (E), and $\text{NO}_3^-\text{-N}$ -enriched (F) conditions. Vertical bars represent \pm SD of the means ($n = 3$).

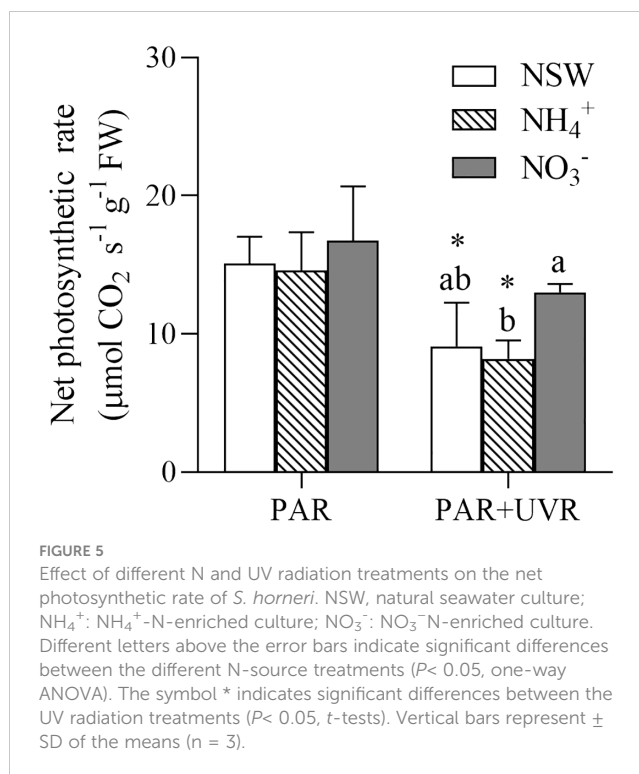
($P < 0.05$) between the groups. However, no significant differences ($P > 0.05$) were observed in the TR_0/RC and ET_0/RC levels of *S. horneri* under various N forms and UV radiation treatments.

3.3 Photosynthetic pigments and UV-absorbing compounds

The results of the two-way analysis of variance indicated that UV radiation had a significant main effect on all three parameters ($P = 0.002$ for Chla, $P = 0.004$ for Car, $P = 0.001$ for UVACs). Under natural seawater culture conditions, PAR+UVR treatments increased the content of Car in the algae (Figure 4). Conversely, this phenomenon was not observed in NH_4^+ -N-enriched or NO_3^- -N-enriched cultures ($P > 0.05$). UV radiation significantly increased the content of UVACs in algae under natural seawater culture and NH_4^+ -N-enriched culture conditions, with increases of 25.67%, 29.73%. UVACs were not significantly affected ($P > 0.05$) by N culture condition under the PAR+UVR radiation treatment.

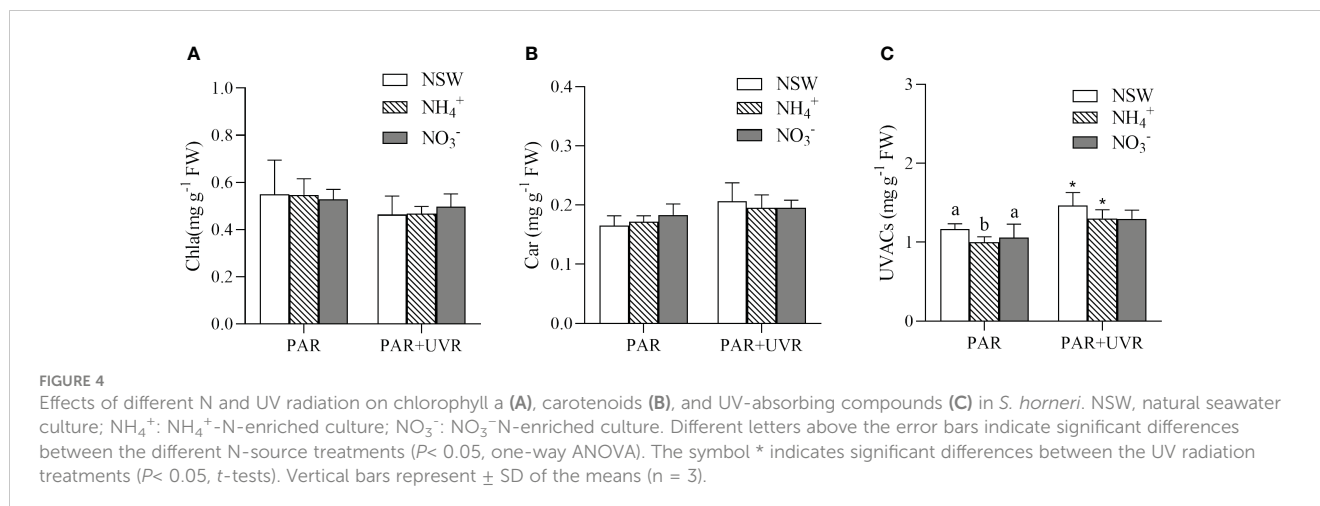
3.4 Net photosynthetic rate

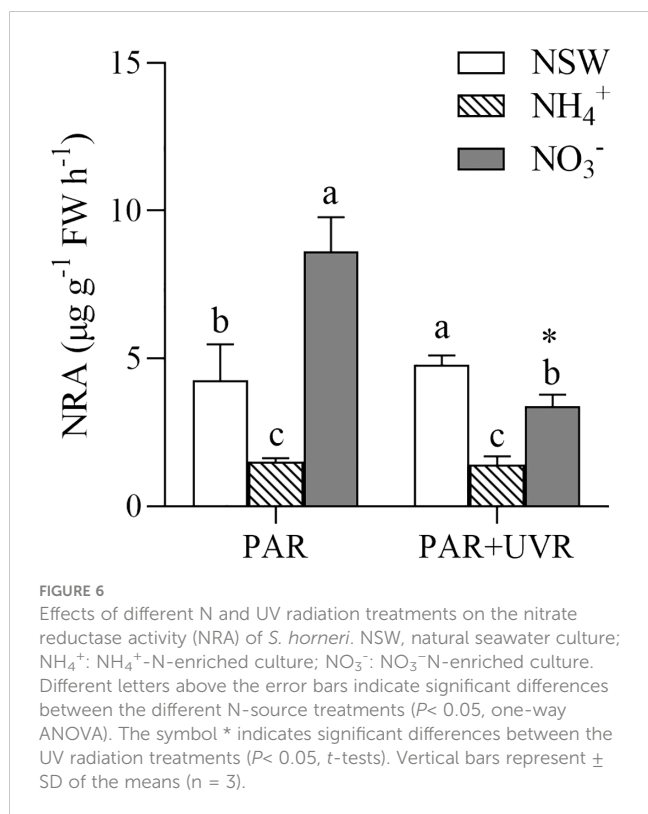
The impact of various N and UV radiation treatments on the net photosynthetic rate of *S. horneri* is depicted in Figure 5. The results of the two-way analysis of variance revealed that only UV radiation had a significant main effect ($P = 0.001$) on the photosynthetic rate. UVR demonstrated a significant ($P < 0.05$) inhibitory effect on the net photosynthetic rate of *S. horneri* in algae under natural seawater culture and NH_4^+ -N-enriched culture conditions. Under the PAR+UVR treatment, the net photosynthetic rate of *S. horneri* was reduced to 60.44%, 56.34%, and 77.69% of the level observed under PAR treatment in natural seawater, NH_4^+ -N-enriched, and NO_3^- -N-enriched cultures, respectively. Additionally, the net photosynthetic rate of *S. horneri* cultured with NO_3^- -N enrichment was significantly higher than that of the NH_4^+ -N enrichment group in the PAR+UVR treatment ($P > 0.05$).



3.5 Nitrate reductase activity

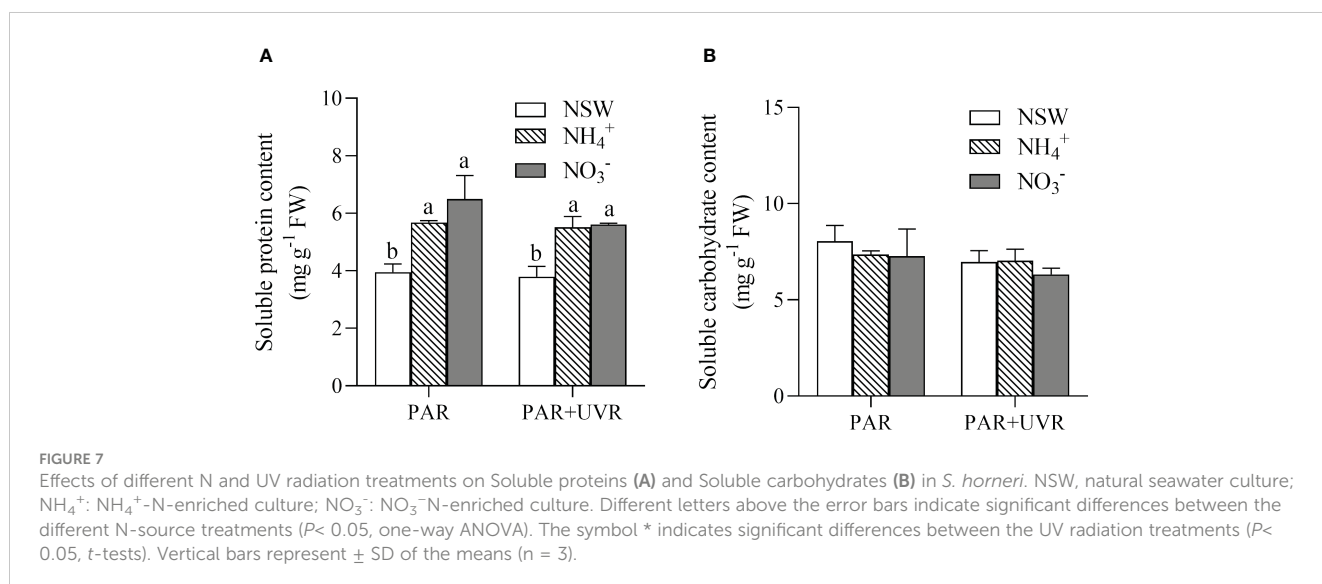
There was an interaction between the UV radiation and N ($P = 0.001$). Notably, NRA of the NH_4^+ -N-enriched cultured *S. horneri* was significantly lower than that of the other N treatments under both UV radiation treatments (Figure 6). Under PAR treatment, the NRA of the NO_3^- -N-enriched cultured alga increased by 102.17% compared that with of the natural seawater. In contrast, the NRA of NH_4^+ -N-enriched cultured alga decreased by 35.44%. Under the PAR+UVR treatment, the NRA of NH_4^+ -N-enriched and NO_3^- -N-enriched cultured alga decreased to 29.32% and 70.61%, respectively, in natural seawater. UVR significantly suppressed the NRA of NO_3^- -N-enriched seawater-cultured *S. horneri* ($P < 0.05$), while this phenomenon was not observed in the other treatments.





3.6 Soluble proteins and soluble carbohydrates

Figure 7 shows the impact of various N and UV radiation treatments on the levels of soluble protein and soluble carbohydrates in *S. horneri*. The results of the two-way analysis of variance indicated that only N had a main effect on soluble protein ($P = 0.001$). Both N enrichments led to significant increases in the level of soluble proteins in algae compared to natural seawater culture, regardless of UV radiation treatments ($P < 0.05$). Neither nitrogen enrichment nor UVR significantly affected the soluble carbohydrate content ($P > 0.05$).



3.7 The main effect of UV radiation and different N source

Figure 8 shows UV radiation have main effect on F_v/F_m , NPQ, Chla, Car, UVACs, and net photosynthetic rate of *S. horneri*. Among them, UV radiation significantly reduced the F_v/F_m and net photosynthetic rate. Meanwhile, Car and UVACs contents were increased by UV radiation.

N-source has a main effect on NPQ and soluble proteins. NPQ in the NH₄⁺ enrichment treatment exhibited the highest value. NO₃⁻ and NH₄⁺ enrichment culture significantly increased the soluble protein content, but there was no difference between them (Figure 9).

4 Discussion

In our previous study, it has been found that *S. horneri* can alleviate the UVR induced stress through several pathways, including accelerated synthesis and interconversion of D1 proteins, enhancement of antioxidant system efficiency (Xu et al., 2022). However, due to the fact that gold tide typically occurs in eutrophic offshore (Smetacek and Zingone, 2013), the impact of high concentrations of nitrogen on UVR effects should not be ignored. In this study, various nitrogen enrichments enhanced the relative growth rate of *S. horneri* (Supplementary Figure S1B). After 2 h UV radiation, the F_v/F_m and net photosynthetic rate of *S. horneri* have been significantly inhibited. Under the condition of nitrogen enrichment, *S. horneri* can resist the damage caused by UVR by increasing NPQ. At different radiation treatments, the enrichments of two nitrogen source showed different photoprotection strategies, indicating that UVR and nitrogen source had significant interaction.

Nitrogen serves as the nutritional foundation and external stimulus for plant development (Crawford, 1995), and elevated nitrogen levels commonly promote macroalgal growth. This study demonstrated that various nitrogen enrichments enhanced the

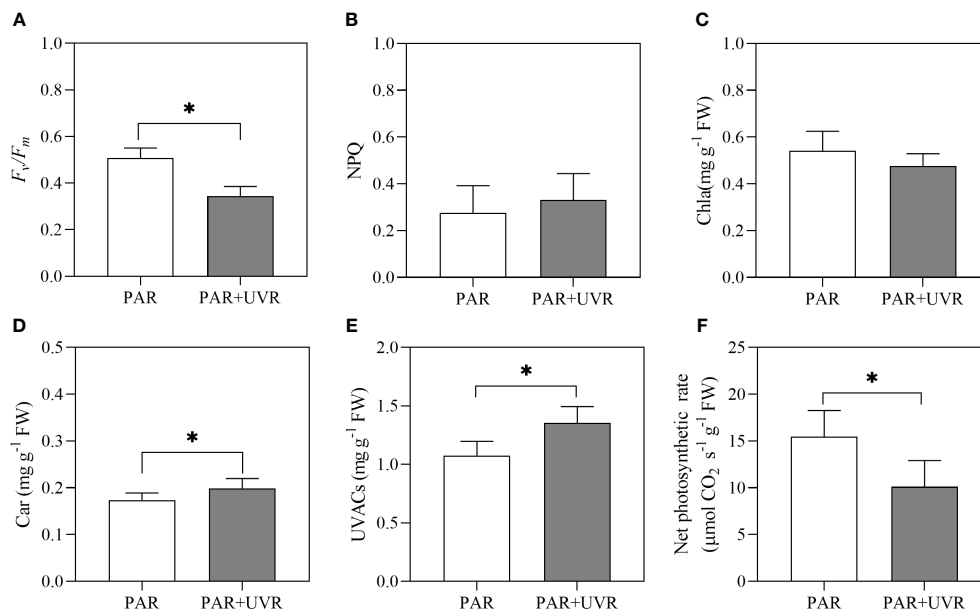


FIGURE 8

Effects of UV radiation on F_v/F_m (A), NPQ (B), Chla (C), Car (D), UVACs (E), and net photosynthetic rate (NPR, F) of *S. horneri*. The symbol * indicates significant differences between the PAR and PAR+UVR treatments ($P < 0.05$, t -tests). Vertical bars represent \pm SD of the means ($n = 9$).

relative growth rate of *S. horneri*. Furthermore, nitrogen source-enriched cultures can increase soluble protein content in the algal body, thereby storing more N sources for the alga (Martínez and Rico, 2008). This may be related to the activity of nitrate reductase (NR), NR is an inducible enzyme, and the availability of substrate nitrate-nitrogen typically enhances its activity (Kaur et al., 2017). Given that nitrate-nitrogen uptake involves the action of nitrate reductase and consumes a substantial amount of energy (Pritchard et al., 2015), ammonia-nitrogen-enriched nitrogen uptake is more energy-efficient, seemingly leading to a potential increase in growth. The soluble carbohydrate content did not increase with increasing N concentration, which may be because algae prioritize protein under N-sufficient conditions, and soluble carbohydrates were

primarily carbon metabolites that were affected by photosynthetic carbon fixation rather than nitrogen.

S. horneri floating on the sea surface may be susceptible to increased levels of UVR. In this study, the F_v/F_m of *S. horneri* in the PAR+UVR radiation treatment was significantly lower than that under the PAR treatment, suggesting that UVR induced strong photoinhibition on *S. horneri*. Nonetheless, compared to *Sargassum muticum*, another species of *Sargassum* genus that have not been observed to form gold tides, the inhibition of UVR on *S. horneri* was relatively mild. The F_v/F_m of *S. muticum* exposed to 2 h UV radiation was more severely reduced (to less than 0.2) (Xu et al., 2023b). UVR radiation mainly damaged water oxidation complexes in the PSII reaction center, where electrons were transferred to P_{680}^+

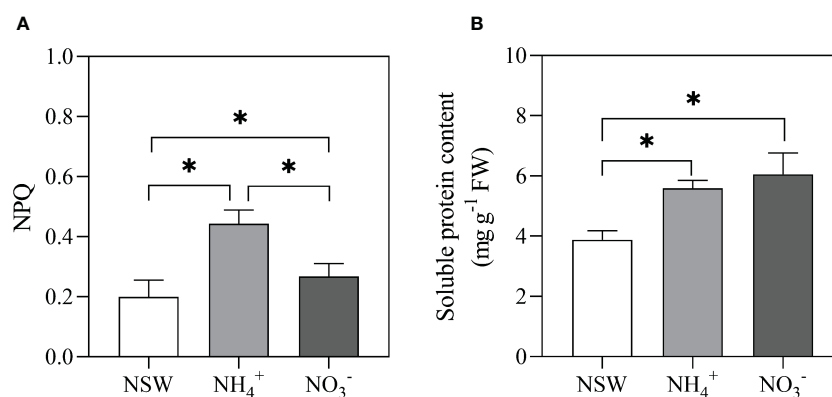


FIGURE 9

Effects of N-source on NPQ (A) and Soluble proteins (SP, B) of *S. horneri*. NSW, natural seawater culture; NH₄⁺: NH₄⁺-N-enriched culture; NO₃⁻: NO₃⁻-N-enriched culture. The symbol * indicates significant differences between the treatments ($P < 0.05$, one-way ANOVA). Vertical bars represent \pm SD of the means ($n = 6$).

(Ivanova et al., 2008), leading to the formation of excessive reactive oxygen species (ROS). Consequently, the transfer of electrons to the secondary electron acceptor Q_A could not be accomplished within the specified time frame, leading to the accumulation of ROS and subsequent damage to algae. Moreover, the oxidized state of the electron acceptor Q_A may degrade pigments, resulting in decreased photosynthetic activity (Sharma et al., 2020). The elevated values of V_j in *S. horneri* subjected to UVR in this study presented an increase in the closure of the active reaction centers. The energy absorbed and dissipated per unit reaction center of *S. horneri* exposed to UVR treatment was significantly higher than that of *S. horneri* exposed to PAR treatment. It has been reported that photosynthetic organisms tend to increase ABS/RC and DI_0/RC to maintain a stable ET_0/RC , thus maintaining the functional integrity of the photosynthetic system when subjected to high excitation energies (Giovagnetti et al., 2014). Therefore, the reduction in the net photosynthetic rate caused by UVR might be attributable to a decrease in the number of active unit reaction centers.

Additionally, the net photosynthetic rate of *S. horneri* enriched in nitrate-nitrogen was greater than that of ammonia-nitrogen-enriched *S. horneri* under UVR. Although the activity of nitrate-nitrogen-enriched NR is significantly reduced by exposure to UVR conditions, but the advantage of nitrate-nitrogen lies in its superior storage capacity. Studies have demonstrated that algal cells can store nitrate-nitrogen in vesicles following uptake. The intracellular and extracellular nitrate-nitrogen concentration ratio can reach 1000:1 (Narvarte et al., 2023), which ensures an ample supply of nitrogen required for other physiological processes such as photosynthesis and carbon fixation in algal cells. Xu and Gao (2012) have reported in *Gracilaria lemaneiformis* that high levels of UVR can disrupt the molecular structure of NR and reduce its activity. However, it has also been shown that NR can absorb UVR, function as a photoreceptor for UVA, and utilize UVA for algal photosynthesis and growth (Gao and Xu, 2008; Xu and Gao, 2009). UVR can act as an environmental factor in controlling the carbon and nitrogen cycles. UVR has been shown to promote NRA in the brown algae *Fucus spiralis* and *Ulva olivascens* (Viñegla et al., 2006). However, the effect of UVR on NRA is species-specific (Huovinen et al., 2007) and depended on the level of UVR. The soluble protein content of nitrogen-enriched *S. horneri* exposed to UVR in this study was lower than that of the visible light treatment, which may be attributable to the inhibition of NR activity.

Macroalgae have evolved protective mechanisms under UV stress. Non-photochemical quenching (NPQ) is a process that converts excess light energy into thermal energy, thereby protecting the PSII reaction centers from UV radiation damage through heat dissipation. This study found that both UV radiation and an increase in nitrogen concentration led to an increase in NPQ in *S. horneri* and that the greater the NPQ, the greater the photoprotective ability of the algae (Goss and Jakob, 2010; Jahns and Holzwarth, 2012). It has been suggested that a higher NPQ is

associated with the accumulation of zeaxanthin (García-Mendoza et al., 2011), which plays a role in the lutein cycle and can either dissipate energy or accelerate the repair of damaged cells in algae (Zudaire and Roy, 2001). In this study, ammonia-nitrogen-enriched cultured *S. horneri* exhibited a higher NPQ and greater photoprotection than nitrate-nitrogen enrichment. This may be due to the facts that NPQ can be rapidly induced in seconds or minutes (García-Mendoza and Colombo-Pallotta, 2007), and ammoniacal nitrogen affects the ΔpH (Ruban et al., 2004). The results of the ammoniacal nitrogen incubation of *S. horneri* ABS/RC and DI_0/RC were significantly lower than those of the other treatments, which may have an indirect effect of increasing excess excitation energy. Carotenoids, which function as antennae pigments, not only capture light energy, but also quench singlet oxygen and other reactive oxygen species (Singh et al., 2010), protecting algal cells from damage. It has been documented that exposure to UVR can induce the synthesis of UV-absorbing compounds (UVACs) in algae (Xu and Gao, 2012; Navarro et al., 2014). In this study, exposure to UVR radiation resulted in increases in the contents both of Car and UVACs in *S. horneri* (Figure 9), which suggested that the alga took protective measures to safeguard its body against UV-induced damage.

5 Conclusion

After the golden tide outbreak, *S. horneri* floating on the surface received more UVR radiation. The findings of this study revealed that exposure to UVR resulted in impairment of the PSII reaction center in *S. horneri*, leading to a decrease in the F_v/F_m and electron transfer rate. Hence, the net photosynthetic carbon fixation rate of *S. horneri* was considerably reduced, ultimately leading to the inhibition of photosynthetic activity. The detrimental effects of UVR were alleviated by amplification of NPQ and accumulation of UV-absorbing substances in algal cells. In this study, exposure of nitrate-enriched cultured *S. horneri* to UVR, ABS/RC, and DI_0/RC was elevated to sustain a stable ET_0/RC . Consequently, the net photosynthetic rate of nitrate-enriched cells was higher than that of ammonia-enriched cultured *S. horneri*. Cultured *S. horneri* enriched with ammonia exhibited a higher rate of NPQ and more robust photoprotective capabilities than cultured *S. horneri* enriched with nitrate. These results may contribute to explaining that the floating *S. horneri* under UVR stress can still form golden tide in eutrophic seawater.

Data availability statement

The original contributions presented in the study are included in the article/Supplementary Material. Further inquiries can be directed to the corresponding authors.

Author contributions

BL: Data curation, Formal analysis, Writing – original draft. ZX: Conceptualization, Funding acquisition, Writing – review & editing. XJ: Methodology, Writing – review & editing. HW: Funding acquisition, Investigation, Writing – review & editing. MB: Funding acquisition, Software, Writing – review & editing. SZ: Formal analysis, Writing – review & editing. FY: Conceptualization, Funding acquisition, Project administration, Supervision, Writing – review & editing. TY: Resources, Supervision, Validation, Visualization, Writing – review & editing.

Funding

The author(s) declare financial support was received for the research, authorship, and/or publication of this article. This work was supported by the National Natural Science Foundation of China (Nos. 42276119, 42376107 and 42206106), and Shandong Provincial Natural Science Foundation of China (No. ZR2023QD091).

References

- Agusti, S., and Llabrés, M. (2007). Solar radiation-induced mortality of marine picoplankton in the oligotrophic ocean. *Photochem. Photobiol.* 83, 793–801. doi: 10.1111/j.1751-1097.2007.00144.x
- Anibal, J., Madeira, H. T., Carvalho, L. F., Esteves, E., Veiga-Pires, C., and Rocha, C. (2014). Macroalgae mitigation potential for fish aquaculture effluents: an approach coupling nitrogen uptake and metabolic pathways using *Ulva rigida* and *Enteromorpha clathrata*. *Environ. Sci. Pollut. Res. Int.* 21, 13324–13334. doi: 10.1007/s11356-013-2427-x
- Bais, A. F., McKenzie, R. L., Bernhard, G., Aucamp, P. J., Ilyas, M., Madronich, S., et al. (2015). Ozone depletion and climate change: impacts on UV radiation. *Photochem. Photobiol. Sci.* 14, 19–52. doi: 10.1039/c4pp90032d
- Bradford, M. M. (1976). A rapid and sensitive method for the quantitation of microgram quantities of protein utilizing the principle of protein-dye binding. *Anal. Biochem.* 72, 248–254. doi: 10.1016/0003-2697(76)90527-3
- Bricker, S. B., Longstaff, B., Dennison, W., Jones, A., Boicourt, K., Wicks, C., et al. (2008). Effects of nutrient enrichment in the nation's estuaries: a decade of change. *Harmful. Algae.* 8, 21–32. doi: 10.1016/j.hal.2008.08.028
- Byeon, S. Y., Oh, H. J., Kim, S., Yun, S. H., Kang, J. H., Park, S. R., et al. (2019). The origin and population genetic structure of the 'golden tide' seaweeds, *Sargassum horneri*, in Korean waters. *Sci. Rep.* 9, 7757. doi: 10.1038/s41598-019-44170-x
- Carmona, R., Kraemer, G. P., and Yarish, C. (2006). Exploring northeast American and Asian species of *Porphyra* for use in an integrated finfish–algal aquaculture system. *Aquaculture* 252, 54–65. doi: 10.1016/j.aquaculture.2005.11.049
- Casele, J. E., Davis, K., and Marks, L. M. (2018). Marine management affects the invasion success of a nonnative species in a temperate reef system in California, USA. *Ecol. Lett.* 21, 43–53. doi: 10.1111/ele.12869
- Corzo, A., and Niell, F. X. (1991). Determination of nitrate reductase activity in *Ulva rigida* C. Agardh by the *in situ* method. *J. Exp. Mar. Biol. Ecol.* 146, 181–191. doi: 10.1016/0022-0981(91)90024-Q
- Crawford, N. M. (1995). Nitrate: nutrient and signal for plant growth. *Plant Cell.* 7, 859–868. doi: 10.1105/tpc.7.7.859
- Dai, W., Wang, X., Zhuang, M., Sun, J., Shen, Y., Xia, Z., et al. (2024). Responses of photosynthesis-related genes in *Sargassum horneri* to high temperature stress. *Mar. Pollut. Bull.* 199, 115944. doi: 10.1016/j.marpolbul.2023.115944
- Davison, I. R., Jordan, T. L., Fegley, J. C., and Grobe, C. W. (2007). Response of *Laminaria saccharina* (Phaeophyta) growth and photosynthesis to simultaneous ultraviolet radiation and nitrogen limitation. *J. Phycol.* 43, 636–646. doi: 10.1111/j.1529-8817.2007.00360.x
- Gao, K., Beardall, J., Häder, D., Hall-Spencer, J. M., Gao, G., and Hutchins, D. (2019). Effects of ocean acidification on marine photosynthetic organisms under the concurrent influences of warming, UV radiation, and deoxygenation. *Front. Mar. Sci.* 6. doi: 10.3389/fmars.2019.00322

Conflict of interest

The authors declare that the research was conducted in the absence of any commercial or financial relationships that could be construed as a potential conflict of interest.

Publisher's note

All claims expressed in this article are solely those of the authors and do not necessarily represent those of their affiliated organizations, or those of the publisher, the editors and the reviewers. Any product that may be evaluated in this article, or claim that may be made by its manufacturer, is not guaranteed or endorsed by the publisher.

Supplementary material

The Supplementary Material for this article can be found online at: <https://www.frontiersin.org/articles/10.3389/fmars.2024.1420839/full#supplementary-material>

- Gao, K., and Xu, J. (2008). Effects of solar UV radiation on diurnal photosynthetic performance and growth of *Gracilaria lemaneiformis* (Rhodophyta). *Eur. J. Phycol.* 43, 297–307. doi: 10.1080/09670260801986837

- García-Mendoza, E., and Colombo-Palotta, M. F. (2007). The giant kelp *Macrocystis pyrifera* presents a different nonphotochemical quenching control than higher plants. *New. Phytol.* 173, 526–536. doi: 10.1111/j.1469-8137.2006.01951.x

- García-Mendoza, E., Ocampo-Alvarez, H., and Govindjee, (2011). Photoprotection in the brown alga *Macrocystis pyrifera*: evolutionary implications. *J. Photochem. Photobiol. B.* 104, 377–385. doi: 10.1016/j.jphotobiol.2011.04.004

- Giovagnetti, V., Flori, S., Tramontano, F., Lavaud, J., and Brunet, C. (2014). The velocity of light intensity increase modulates the photoprotective response in coastal diatoms. *PLoS. One* 9, e103782. doi: 10.1371/journal.pone.0103782

- Goss, R., and Jakob, T. (2010). Regulation and function of xanthophyll cycle-dependent photoprotection in algae. *Photosynth. Res.* 106, 103–122. doi: 10.1007/s11120-010-9536-x

- Goss, R., and Lepetit, R. (2015). Biodiversity of NPQ. *J. Plant Physiol.* 172, 13–32. doi: 10.1016/j.jplph.2014.03.004

- Helbling, E. W., Barbieri, E. S., Sinha, R. P., Villafañe, V. E., and Häder, D. P. (2004). Dynamics of potentially protective compounds in Rhodophyta species from Patagonia (Argentina) exposed to solar radiation. *J. Photochem. Photobiol. B.* 75, 63–71. doi: 10.1016/j.jphotobiol.2004.05.006

- Huovinen, P., Gómez, I., and Orostegui, M. (2007). Patterns and UV sensitivity of carbon anhydrase and nitrate reductase activities in south Pacific macroalgae. *Mar. Biol.* 151, 1813–1821. doi: 10.1007/s00227-007-0613-4

- Hwang, E. K., Lee, S. J., Ha, D. S., and Park, C. S. (2016). *Sargassum* golden tides in the Shinan-gun and Jeju Island, Korea. *Korean. J. Fish. Aquat. Sci.* 49, 689–693. doi: 10.5657/KFAS.2016.0689

- Hwang, R. L., Tsai, C. C., and Lee, T. M. (2004). Assessment of temperature and nutrient limitation on seasonal dynamics among species of *Sargassum* from a coral reef in southern Taiwan. *J. Phycol.* 40, 463–473. doi: 10.1111/j.1529-8817.2004.03086.x

- Ivanova, P. I., Dobrikova, A. G., Taneva, S. G., and Apostolova, E. L. (2008). Sensitivity of the photosynthetic apparatus to UV-A radiation: role of light-harvesting complex II-photosystem II supercomplex organization. *Radiat. Environ. Bioph.* 47, 169–177. doi: 10.1007/s00411-007-0139-7

- Jahns, P., and Holzwarth, A. R. (2012). The role of the xanthophyll cycle and of lutein in photoprotection of photosystem II. *BBA-Bioenergetics.* 1817, 182–193. doi: 10.1016/j.bbabi.2011.04.012

- Kaur, B., Kaur, G., and Asthir, B. (2017). Biochemical aspects of nitrogen use efficiency: An overview. *J. Plant Nutr.* 40, 506–523. doi: 10.1080/01904167.2016.1240196

- Kochert, G. (1978). "Carbohydrate determination by the phenol-sulfuric acid method," in *Handbook of Physiological Methods: Physiological and Biochemical Methods* (Cambridge University Press, London, New York, Melbourne), 92–93.
- Komatsu, T., Mizuno, S., Natheer, A., Kantachumpoo, A., Tanaka, K., Morimoto, A., et al. (2014). Unusual distribution of floating seaweeds in the East China Sea in the early spring of 2012. *J. Appl. Phycol.* 26, 1169–1179. doi: 10.1007/s10811-013-0152-y
- Lacour, T., Robert, E., and Lavaud, J. (2023). Sustained xanthophyll pigments-related photoprotective NPQ is involved in photoinhibition in the haptophyte *Tisochrysis lutea*. *Sci. Rep.* 13, 14694. doi: 10.1038/s41598-023-40298-z
- Liu, F., Liu, X., Wang, Y., Jin, Z., Moejes, F. W., and Sun, S. (2018). Insights on the *Sargassum horneri* golden tides in the Yellow Sea inferred from morphological and molecular data. *Limnol. Oceanogr.* 63, 1762–1773. doi: 10.1002/lno.10806
- Martinez, B., and Rico, J. M. (2008). Changes in nutrient content of *Palmaria palmate* in response to variable light and upwelling in northern Spain. *J. Phycol.* 44, 50–59. doi: 10.1111/j.1529-8817.2007.00440.x
- Mayalen, Z., Marie, S. F., Véronique, K., Klervi, L. L., Valérie, S.-P., Marilyne, F., et al. (2009). Antioxidant and antitumoural activities of some Phaeophyta from Brittany coasts. *Food. Chem.* 16, 693–701. doi: 10.1016/j.foodchem.2009.03.025
- Narvarte, B. C. V., Hinaloc, L. A. R., Gonzaga, S. M. C., Crisostomo, B. A., Genovia, T. G. T., and Roleda, M. Y. (2023). Nitrate and phosphate uptake of morphologically distinct calcified macroalgae. *Phycologia* 62, 551–560. doi: 10.1080/00318884.2023.2197636
- Navarro, N., Mansilla, A., Figueroa, F., Korbee, N., Jofre, J., and Plastino, E. (2014). Short-term effects of solar UV radiation and NO₃ supply on the accumulation of mycosporine-like amino acids in *Pyropia columbina* (Bangiales, Rhodophyta) under spring ozone depletion in the subAntarctic region, Chile. *Bot. Mar.* 57, 9–20. doi: 10.1515/bot-2013-0090
- Neori, A., Chopin, T., Troell, M., Buschmann, A. H., Kraemer, G. P., Halling, C., et al. (2004). Integrated aquaculture: rationale, evolution and state of the art emphasizing seaweed biofiltration in modern mariculture. *Aquaculture* 231, 361–391. doi: 10.1016/j.aquaculture.2003.11.015
- Paliwal, C., Mitra, M., Bhayani, K., Bharadwaj, S. V. V., Ghosh, T., Dubey, S., et al. (2017). Abiotic stresses as tools for metabolites in microalgae. *Bioresour. Technol.* 244, 1216–1226. doi: 10.1016/j.biortech.2017.05.058
- Pritchard, D. W., Hurd, C. L., Beardall, J., and Hepburn, C. D. (2015). Restricted use of nitrate and a strong preference for ammonium reflects the nitrogen ecophysiology of a light-limited red alga. *J. Phycol.* 51, 277–287. doi: 10.1111/jpy.12272
- Qi, L., Hu, C., Wang, M., Shang, S., and Wilson, C. (2017). Floating Algae Blooms in the East China Sea. *Geophys. Res. Lett.* 44, 501–511. doi: 10.1002/2017GL075525
- Rautio, M., and Tartarotti, B. (2010). UV radiation and freshwater zooplankton: damage, protection and recovery. *Freshw. Rev.* 3, 105–131. doi: 10.1608/FRJ-3.2.157
- Ruban, A., Lavaud, J., Rousseau, B., Guglielmi, G., Horton, P., and Etienne, A. L. (2004). The super-excess energy dissipation in diatom algae: comparative analysis with higher plants. *Photosynth. Res.* 82, 165–175. doi: 10.1007/s11120-004-1456-1
- Ruhland, C. T., Fogal, M. J., Buyarski, C. R., and Krna, M. A. (2007). Solar ultraviolet-B radiation increases phenolic content and ferric reducing antioxidant power in *Avena sativa*. *Molecules* 12, 1220–1232. doi: 10.3390/12061220
- Schell, J. M., Goodwin, D. S., and Siuda, A. N. S. (2015). Recent *Sargassum* inundation events in the Caribbean: Shipboard observations reveal dominance of a previously rare form. *Oceanography* 28, 8–10. doi: 10.5670/oceanog.2015.70
- Schmidt, É.C., Nunes, B. G., and Maraschin, M. (2010). Effect of ultraviolet-B radiation on growth, photosynthetic pigments, and cell biology of *Kappaphycus alvarezii* (Rhodophyta, Gigartinales) macroalgae brown strain. *Photosynthetica* 48, 161–172. doi: 10.1007/s11099-010-0022-7
- Sfriso, A., and Facca, C. (2013). Annual growth and environmental relationships of the invasive species *Sargassum muticum* and *Undaria pinnatifida* in the lagoon of Venice. *Estuar. Coast. Shelf. S.* 129, 162–172. doi: 10.1016/j.ecss.2013.05.031
- Sharma, A., Kumar, V., Shahzad, B., Ramakrishnan, M., Sidhu, G., Bali, A., et al. (2020). Photosynthetic response of plants under different abiotic stresses: A review. *J. Plant Growth. Regul.* 39, 509–531. doi: 10.1007/s00344-019-10018-x
- Singh, S. P., Häder, D. P., and Sinha, R. P. (2010). Cyanobacteria and ultraviolet radiation (UVR) stress: mitigation strategies. *Ageing. Res. Rev.* 9, 79–90. doi: 10.1016/j.arr.2009.05.004
- Smetacek, V., and Zingone, A. (2013). Green and golden seaweed tides on the rise. *Nature* 504, 84–88. doi: 10.1038/nature12860
- Sobrino, C., Montero, O., and Lubián, L. M. (2004). UV-B radiation increases cell permeability and damages nitrogen incorporation mechanisms in *Nannochloropsis gaditana*. *Aquat. Sci.* 66, 421–429. doi: 10.1007/s00027-004-0731-8
- Solomon, S., Ivy, D. J., Kinnison, D., Mills, M. J., Neely, R. R., and Schmidt, A. (2016). Emergence of healing in the Antarctic ozone layer. *Science* 353, 269–274. doi: 10.1126/science.aac0061
- Song, W., Li, Z., Liu, F., Ding, Y., Qi, P., You, H., et al. (2018). Effective removal of ammonia nitrogen from waste seawater using crystal seed enhanced struvite precipitation technology with response surface methodology for process optimization. *Environ. Sci. Pollut. Res.* 25, 628–638. doi: 10.1007/s11356-017-0441-0
- Strasser, R. J., Srivastava, A., and Tsimilli-Michael, M. (2000). "The fluorescence transient as a tool to characterize and screen photosynthetic samples," in *Probing Photosynthesis: Mechanism, Regulation and Adaptation*, vol. 25. Eds. M. Yunus, U. Pathre and P. Mohanty (Taylor and Francis Press, London), 445–483.
- Sun, K. M., Li, R., Li, Y., Xin, M., Xiao, J., Wang, Z., et al. (2015). Responses of *Ulva prolifera* to short-term nutrient enrichment under light and dark conditions. *Estuar. Coast. Shelf. S.* 163, 56–62. doi: 10.1016/j.ecss.2015.03.018
- Tedetti, M., and Sempéré, R. (2006). Penetration of ultraviolet radiation in the marine environment. A review. *Photochem. Photobiol.* 82, 389–397. doi: 10.1562/2005-11-09-IR-733
- Terawaki, T., Yoshikawa, K., Yoshida, G., Uchimura, M., and Iseki, K. (2003). Ecology and restoration techniques for sargassum beds in the seto inland Sea, Japan. *Mar. Pollut. Bull.* 47, 198–201. doi: 10.1016/S0025-326X(03)00054-7
- Van Tussenbroek, B. I., Hernández Arana, H. A., Rodríguez-Martínez, R. E., Espinoza-Avalos, J., Canizales-Flores, H. M., González-Godoy, C. E., et al. (2017). Severe impacts of brown tides caused by *Sargassum* spp. on near-shore Caribbean seagrass communities. *Mar. Pollut. Bull.* 122, 272–281. doi: 10.1016/j.marpolbul.2017.06.057
- Viñeola, B., Segovia, M., and Figueroa, F. L. (2006). Effect of artificial UV radiation on carbon and nitrogen metabolism in the macroalgae *Fucus spiralis* L. and *Ulva olivascens* Dangard. *Hydrobiologia* 560, 31–42. doi: 10.1007/s10750-005-1097-1
- Wang, M., Hu, C., Barnes, B. B., Mitchum, G., Lapointe, B., and Montoya, J. P. (2019). The great Atlantic *Sargassum* belt. *Science* 365, 83–87. doi: 10.1126/science.aaw7912
- Williams, A., and Feagin, R. (2010). *Sargassum* as a natural solution to enhance dune plant growth. *Environ. Manage.* 46, 738–747. doi: 10.1007/s00267-010-9558-3
- Witze, A. (2020). Rare ozone hole opens over Arctic - and it's big. *Nature* 580, 18–19. doi: 10.1038/d41586-020-00904-w
- Wu, H., Cockshutt, A. M., McCarthy, A., and Campbell, D. A. (2011). Distinctive photosystem II photoinactivation and protein dynamics in marine diatoms. *Plant Physiol.* 156, 2184–2195. doi: 10.1104/pp.111.178772
- Xiao, J., Wang, Z., Liu, D., Fu, M., Yuan, C., and Yan, T. (2021). Harmful macroalgal blooms (HMBs) in China's coastal water: Green and golden tides. *Harmful. Algae* 107, 102061. doi: 10.1016/j.hal.2021.102061
- Xing, Q., Guo, R., Wu, L., An, D., Cong, M., Qin, S., et al. (2017). High-resolution satellite observations of a New Hazard of golden tides caused by floating *Sargassum* in winter in the Yellow Sea. *IEEE. Geosci. Remote. S.* 14, 1815–1819. doi: 10.1109/LGRS.2017.2737079
- Xu, Z., and Gao, K. (2009). Impacts of UV radiation on growth and photosynthetic carbon acquisition in *Gracilaria lemaneiformis* (Rhodophyta) under phosphorus-limited and replete conditions. *Funct. Plant Biol.* 36, 1057–1064. doi: 10.1071/FP09092
- Xu, Z., and Gao, K. (2012). NH₄⁺ enrichment and UV radiation interact to affect the photosynthesis and nitrogen uptake of *Gracilaria lemaneiformis* (Rhodophyta). *Mar. Pollut. Bull.* 64, 99–105. doi: 10.1016/j.marpolbul.2011.10.016
- Xu, Z., Jiang, X., Li, B., Lv, Z., Wu, H., Zang, S., et al. (2023a). Effects of UVR on photosynthesis in *sargassum horneri* (Turner) C. Agardh adapted to different nitrogen levels. *J. Mar. Sci. Eng.* 11, 498. doi: 10.3390/jmse11030498
- Xu, Z., Li, L., Jiang, H., Yan, F., Liu, L., Zang, S., et al. (2022). Photosynthetic responses of a golden tide alga (*Sargassum horneri*) to ultraviolet radiation. *Front. Mar. Sci.* 9. doi: 10.3389/fmars.2022.978376
- Xu, Z., Li, B., Li, L., Wang, N., Wang, Y., Yan, F., et al. (2023b). Effects of UV radiation on photosynthesis of *Sargassum muticum*. *J. Exp. Mar. Biol. Ecol.* 569, 151961. doi: 10.1016/j.jembe.2023.151961
- Zhang, J., Ding, X., Zhuang, M., Wang, S., Chen, L., Shen, H., et al. (2019). An increase in new *Sargassum* (Phaeophyceae) blooms along the coast of the East China Sea and Yellow Sea. *Phycologia* 58, 374–381. doi: 10.1080/00318884.2019.1585722
- Zhuang, M., Liu, J., Ding, X., He, J., Zhao, S., Wu, L., et al. (2021). *Sargassum* blooms in the East China Sea and Yellow Sea: Formation and management. *Mar. Pollut. Bull.* 162, 111845. doi: 10.1016/j.marpolbul.2020.111845
- Zudaire, L., and Roy, S. (2001). Photoprotection and long-term acclimation to UV radiation in the marine diatom *Thalassiosira weissflogii*. *J. Photochem. Photobiol. B.* 62, 26–34. doi: 10.1016/S1011-1344(01)00150-6